

#### 4.1 Introduction

This chapter examines the hybridization of an existing sub-critical coal-fired power plant (CFPP) with concentrated solar thermal energy on technical, environmental, and economic criteria under three different integration scenarios. In this study, a solar field consisting of PTC arrays is integrated with an existing 330 MW sub-critical CFPP for feedwater preheating. The economic factors (*ACoE*, *LCoE*, and simple payback period) and the environmental factors such as annual reductions in coal consumption, CO<sub>2</sub> emissions, and solar contribution have been computed and discussed in this chapter. Exergetic analysis is also performed in this study.

#### 4.2 System Description

In India, the energy consumed for different applications, either domestic or industrial, primarily originates from coal. Therefore, the hybridization of solar energy with existing CFPP has profound and realistic implications. A 330 MW coal-fired sub-critical thermal power plant (*TPP*) is chosen as a reference plant for establishing the integration of solar thermal energy (*STE*) into an existing conventional CFPP. The plant under study is located in Gujarat, India. The *TPP*'s main components are condenser, boiler, turbine, generator, FWHs, and pumps. Its turbine max continuous rating (*TMCR*) capacity is 335 MW as per the heat balance sheet. Hence, all the calculations are out for 335 MW. In the original CFPP, the coal-fired boiler provides steam to a multi-stage turbine-generator, and after expansion, the exhaust steam goes into a condenser at a vacuum. After that, the condensate goes through

several feedwater heaters (*FWHs*), which use extracted steam from higher pressure stages of the turbine till the final feed water temperature is increased to the design value. This cycle is generally referred to as regenerative feed water heating, providing high cycle efficiency. The original CFPP cycle consists of two series of *FWHs*: LP Heaters (*DJ*) and HP Heaters (*GJ*) as shown in Figure 4.1. The main parameters of extraction steam are shown in Table 4.1.

Before the integration of CFPP with solar energy, the unsaturated feed water from the condenser enters into the boiler after going through the four LP *FWHs* (*DJ6*, *DJ5*, *DJ4*, and *DJ3*), a deaerator (*DEA*), and two HP *FWHs* (*GJ2* and *GJ1*). The deaerator is an open type *FWH*, and its purpose is to preheat the feedwater and remove the dissolved gases. The *FWHs* are closed-type heaters. The investigated CFPP has seven steam extraction stages: one stage in HP, three in IP, and three in LP turbine (Figure 4.1). The extracted steam from the turbine is used to preheat feedwater, increasing the plant's overall thermal efficiency. The superheated steam from the superheater passes through the turbine's HP stage and is then reheated in the boiler. After that, the reheated steam enters into the IP and the LP turbines, which finally exhausts in the condenser.

After hybridization, a solar-driven *FWH* is added parallel to the first-stage heater (*GJ1*), as shown in Figure 4.2. When the solar insolation is adequate, extracted steam from HP turbine is cut off, and the feedwater entering high-pressure *FWH* (*GJ1*) is heated in the solar-driven *FWH*. When solar insolation is inadequate to replace the extracted steam completely, the feed water's total flow at the inlet of high-pressure *FWH* (*GJ1*) is divided into two parts. One part is introduced into *FWH* *GJ1*, while the other one flows into the solar *FWH*. Thus, the feed water can be heated by both the extracted steam from the turbine and the concentrated solar energy simultaneously. The temperature of feed water at outlet of *FWH* and the *FWH* *GJ1* can reach the required inlet temperature of the boiler by varying the flow rate of both the feed water and the thermic oil into the solar collectors.

Similarly, after integrating CFPP with STE, the bled-off steam from various stages of turbines is partly or entirely substituted by a solar-driven FWH that is arranged in parallel with one or more stages of FWHs. In the present investigation, integration of concentrated solar power system with FWHs is considered, and three different replacement scenarios are presented and discussed, as follows:

- High-pressure FWH No.1 (*GJ1*) is substituted by solar field, as shown in Figure 4.2.
- High-pressure FWH No. 2 (*GJ2*) is substituted by solar field, as shown in Figure 4.3.
- Both high-pressure FWHs (*GJ1* & *GJ2*) are substituted by solar field, as shown in Figure 4.4.

As stated above in Option-1, the extraction steam from HP turbine is cut off, and the feedwater is preheated by the solar field added in parallel to FWH No.1 up to the required inlet temperature. In Option-2, the 1<sup>st</sup> stage extraction steam from IP turbine is cut off, and the feedwater is preheated by the solar field added in parallel to FWH No. 2 up to the required inlet temperature. In Option-3, the extraction steam from both HP and IP turbine are cut off, and the feedwater is preheated by the solar field added in parallel to FWHs (*GJ1* & *GJ2*) up to the required inlet temperature. Such integration will lead to the requirement of reduced steam to generate the rated amount of electricity, and thus coal can be saved in a fuel-saving approach. And in the power-boosting approach, such hybridization will lead to augmented power output, keeping the same coal consumption.

Several studies reviewed in the literature survey deduced that the most efficient position for integrating solar energy in the coal based power plant is at the highest possible pressure FWHs. Therefore, in this study, a solar collector field comprising of PTC array is used to replace the steam extracted from HP and IP turbines.

### 4.3 Postulates

The succeeding guesses are considered for the present investigation:

- The integrated plant under study is assumed to operate at full load and at turbine maximum condition rating.
- For a particular FWH under examination, the STE substitutes bled steam completely.
- For remaining FWHs, normal feedwater regeneration using turbine bled steam (*TBS*) continues.
- When feedwater heating is undergoing in a specific FWH using solar energy, the rise in feedwater temperature across the FWH will be equal to the temperature reached in the Option of regeneration through TBS.
- During feedwater heating using solar energy, it is supposed that only sensible heating of working fluid and HTF takes place.
- When feedwater heating is done using solar energy in a specific heater, the mass flow rates of extraction steam supplied to other FWHs will vary and can be obtained through first law analysis.
- All calculations are based on steady-state conditions. The temperatures and pressures of steam in the cycle at all points are assumed to be unchanging.
- Three hundred sunny days in a year and 8 hours of daily sunshine are considered in this study.
- DNI is assumed as  $500 \text{ W/m}^2$ , and the efficiency of solar collectors is considered as 60% (Ahmadi et al. 2017).
- HTF considered in this study is Therminol VP-1.

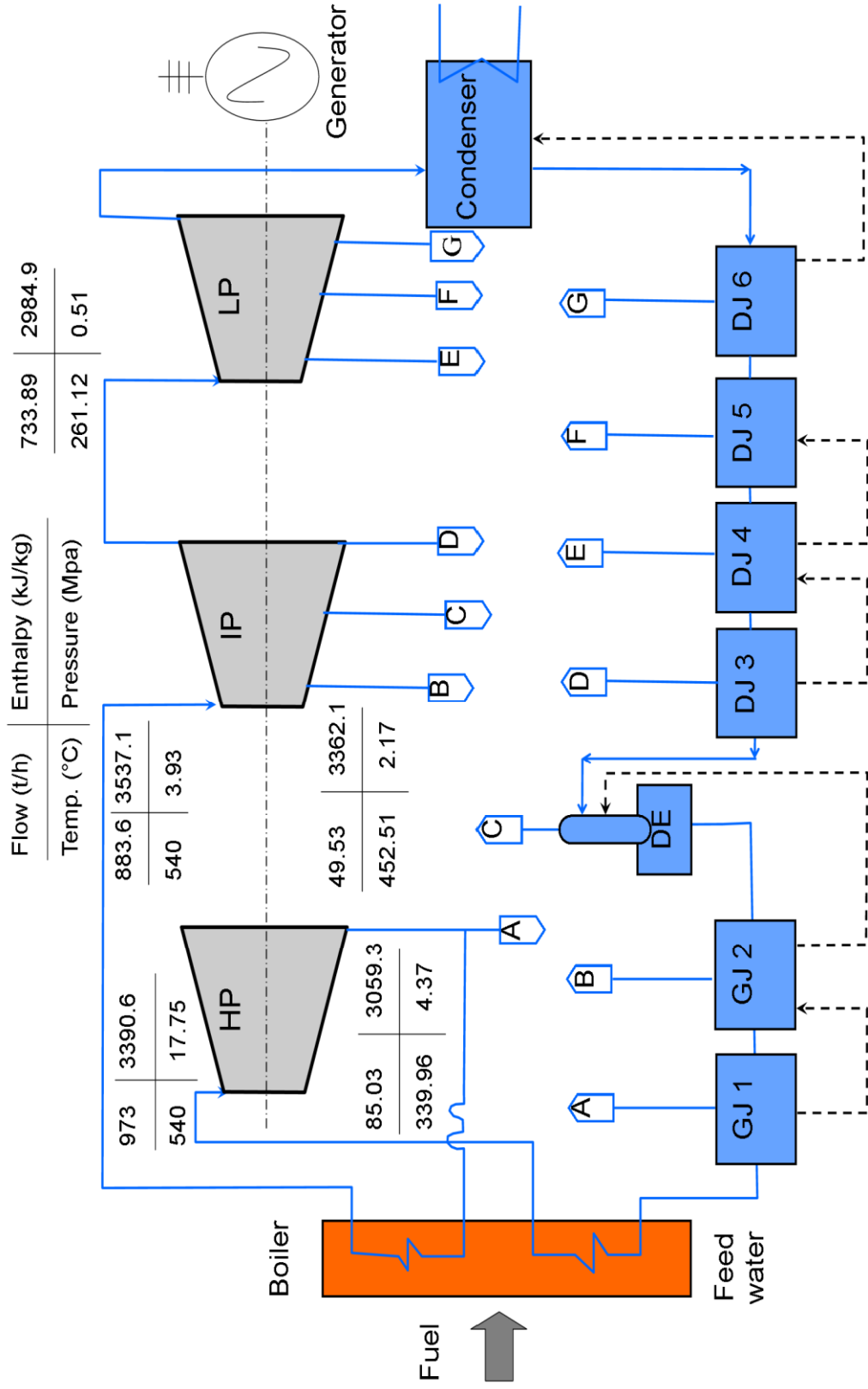


Figure 4.1: Representation of reference plant of 330 MWe original CFPP (Base Option).

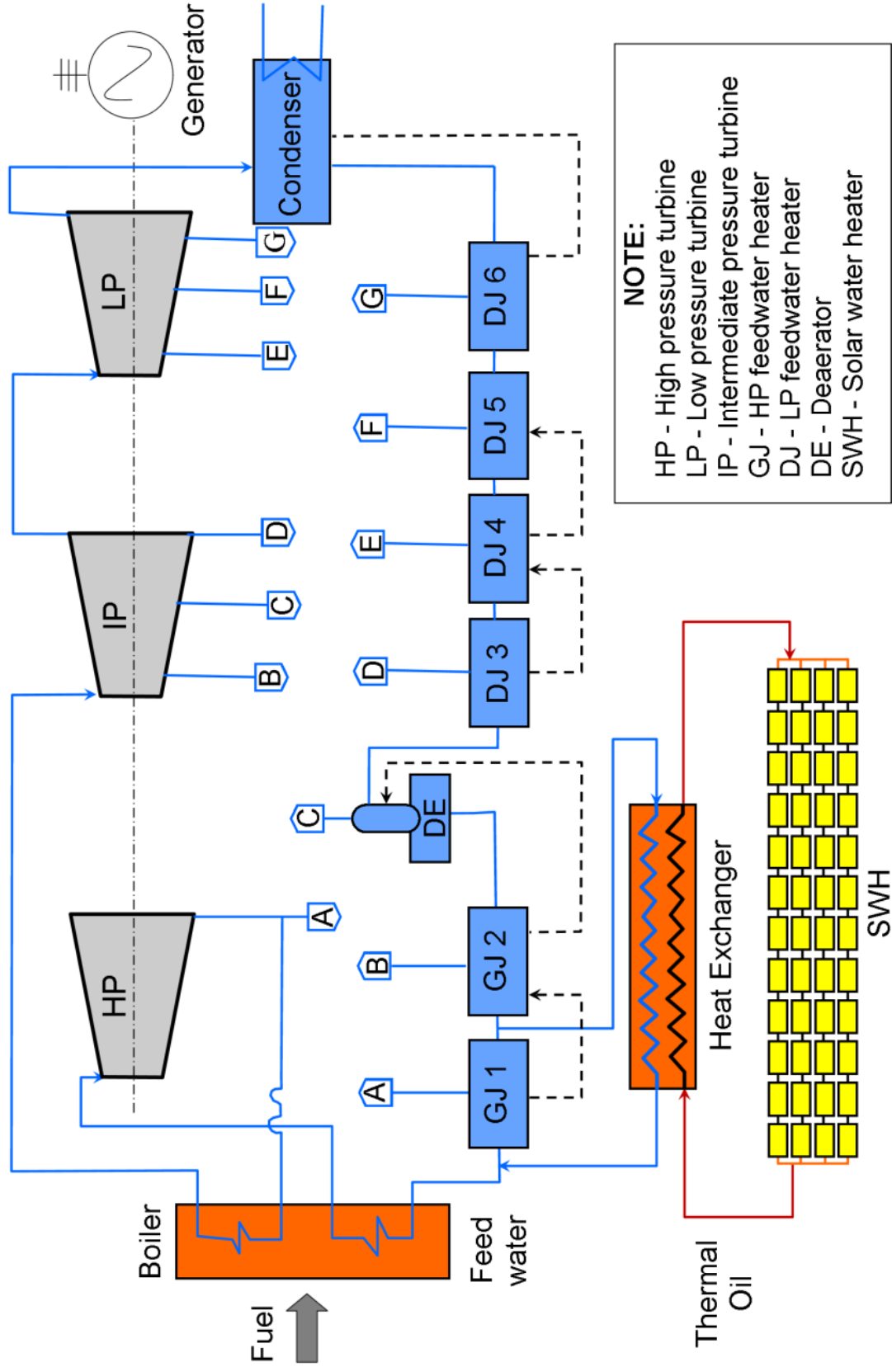


Figure 4.2: Representation of 330 MWe “Solar-coal hybrid power plant” (Option-I).

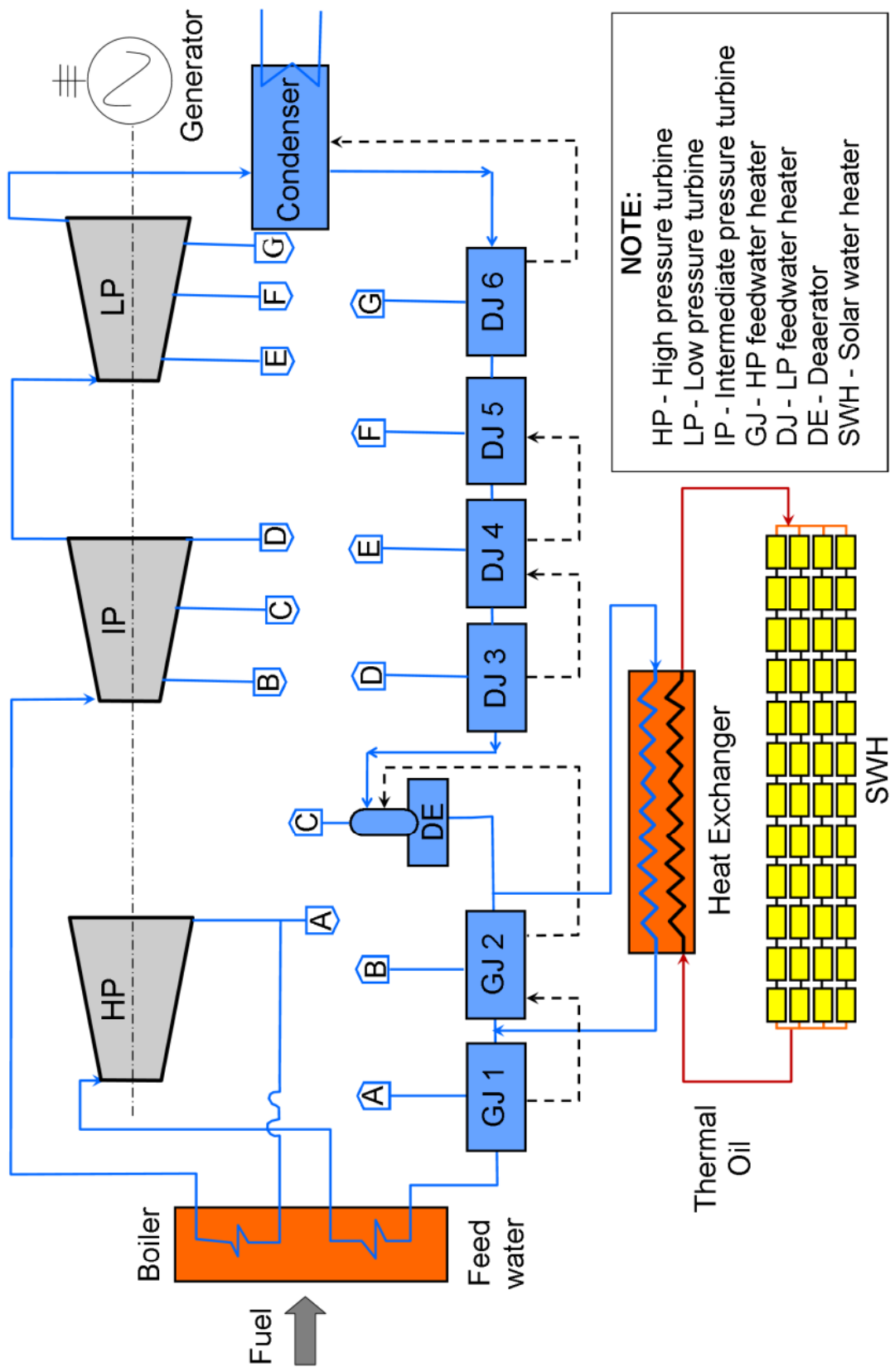


Figure 4.3: Representation of 330 MWe “Solar-coal hybrid power plant” (Option-2).

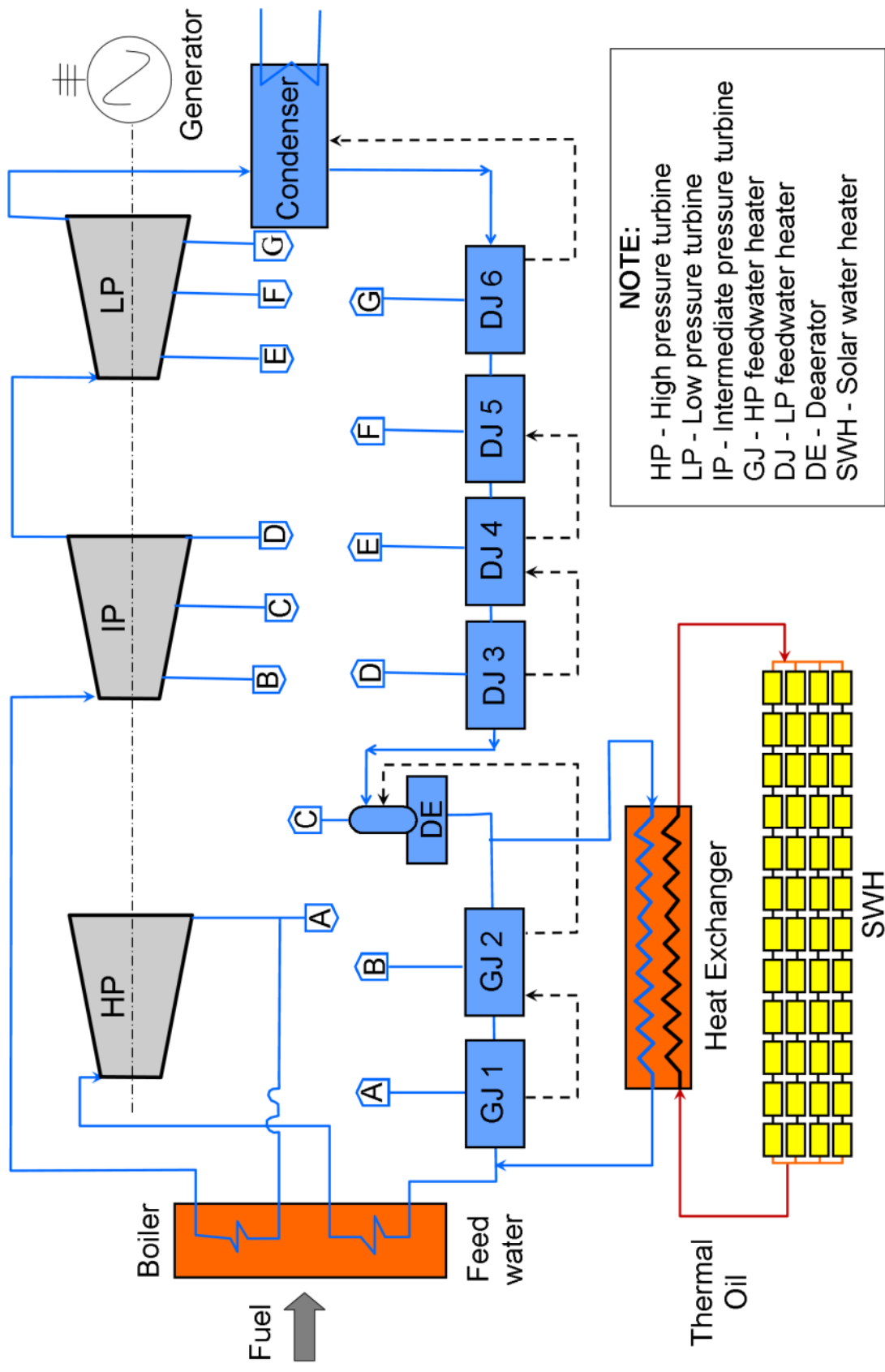


Figure 4.4: Representation of 330MWe “Solar-coal hybrid power plant” (Option-3).



**Table 4.1:****Extraction steam main parameters of reference plant**

<b>Steam Extraction</b>	<b>P<sub>s</sub> (MPa)</b>	<b>T<sub>s</sub> (°C)</b>	<b>h<sub>s</sub> (kJ/kg)</b>	<b>m<sub>s</sub> (Ton/h)</b>	<b>h<sub>w</sub> (kJ/kg)</b>
<b>Primary Steam</b>	17.75	540.00	3390.6	973.00	-
<b>GJ 1</b>	4.3723	339.96	3059.3	85.03	1095.1
<b>GJ 2</b>	2.1724	452.51	3362.1	49.53	939.7
<b>DEA</b>	1.0674	353.50	3165.6	43.56	818.7
<b>DJ 3</b>	0.5063	261.12	2984.9	54.53	630.6
<b>DJ 4</b>	0.1393	136.76	2746.9	23.12	472.6
<b>DJ 5</b>	0.0713	90.43	2639.8	27.53	394.1
<b>DJ 6</b>	0.0292	68.50	2515.0	22.91	271.1
<b>Exhaust Steam</b>	0.0097	45.24	2382.2	660.95	189.4

#### 4.4 Solar Collector Field and Performance Parameters

In this study, PTC solar technology is considered for integrating STE into a conventional coal-based power plant. The DNI data for the location of the plant understudy for a TMY is obtained from NREL's "System Advisor Model (SAM) library (Source: <https://sam.nrel.gov/>,"). The variation of DNI for all the months of a TMY has been shown in Figure 4.5. The details of geometrical and optical parameters of PTC solar field are presented in Table 4.2. Therminol VP-1 is HTF in "oil-water heat exchanger".

##### 4.4.1 Energy parameters

The various energy performance parameters of the solar-coal hybrid TPP are calculated. The input energy to the solar field ( $\dot{Q}_s$ ) and the output energy of the PTC solar field ( $\dot{Q}_c$ ) are

evaluated using equations 3.25 and 3.26, respectively, as discussed in Chapter-3. In this study, the collection efficiency of PTC is taken as 60% (Pai 1991).

The collector area needed to transfer the required output energy is evaluated using equation 3.27 given in Chapter-3. Plant energy efficiency ( $\eta_I$ ) is calculated using equation 3.28 as described in Chapter-3. The energy performance index ( $EnPI$ ) in power boosting mode is defined according to equation 3.29. The solar contribution (%) is obtained using equation 3.30.

#### 4.4.2 Exergy parameters

The exergy performance parameters of the solar-coal hybrid TPP is calculated as per following. In this study, the reference plant uses imported Indonesian coal as the primary energy source, which is assumed to have a gross calorific value ( $GCV$ ) of 21767.2 kJ/kg (Gupta and Srivastav 2010). The specific exergy ( $\psi_c$ ) of coal in MJ/kg is calculated using equation 4.1 (Zhai et al. 2013).

$$\psi_c = GCV + 340.05181(C) - 831.916575(H) + 477.8328(O) + 5.25(N) + 2237.1669(S) - 48.81534(Ash) \quad (4.1)$$

Plant exergy efficiency is obtained using equation 4.2 (Adibhatla and Kaushik 2017) as follows:

$$\eta_{II} = \frac{\dot{W}_{net}}{\dot{m}_f \times \psi_c} \quad (4.2)$$

Here  $\dot{W}_{net}$  is the net electric output of the reference plant (MWe) and  $\dot{m}_f$ , is the mass flow rate of coal in kg/s. The exergy input through solar radiation ( $\dot{E}_{xs}$ ) can be calculated using the

equation 4.3 (Hu et al. 2010).

$$\dot{E}_{xs} = \left[ 1 - \frac{4T_a}{3T_{sun}} (1 - 0.28 \ln f) \right] \times \dot{Q}_s \quad (4.3)$$

Where  $T_a$  is the ambient temperature (298 K),  $T_{sun}$  is the temperature of the Sun (5777 K), and ' $f$ ' is the dilution factor ( $1.3 \times 10^{-5}$ ). The exergy performance index ( $ExPI$ ) can be evaluated using equation 4.4. Here  $\Delta P_{excess}$  is the extra power generated over rated capacity in MW (Suresh et al. 2010).

$$ExPI = \frac{\Delta P_{excess}}{\dot{E}_{xs}} \quad (4.4)$$

**Table 4.2:**

**PTC Field - Geometrical and optical parameters**

<b>Parameters</b>	<b>Specifications</b>	<b>Unit</b>
Outer diameter of the absorber tube	0.07	m
Inner diameter of the absorber tube	0.066	m
Outer diameter of the glass envelope	0.12	m
Inner diameter of the glass envelope	0.115	m
Number of modules/collector	12	-
Each module length	12.27	m
Length of the mirror in each module	11.9	m
Focal length	1.71	m
Width of aperture	5.77	m
Intercept factor	92%	-
Reflectivity of mirror	92%	-
Transmissivity of glass	94.5%	-
Absorptivity	94%	-

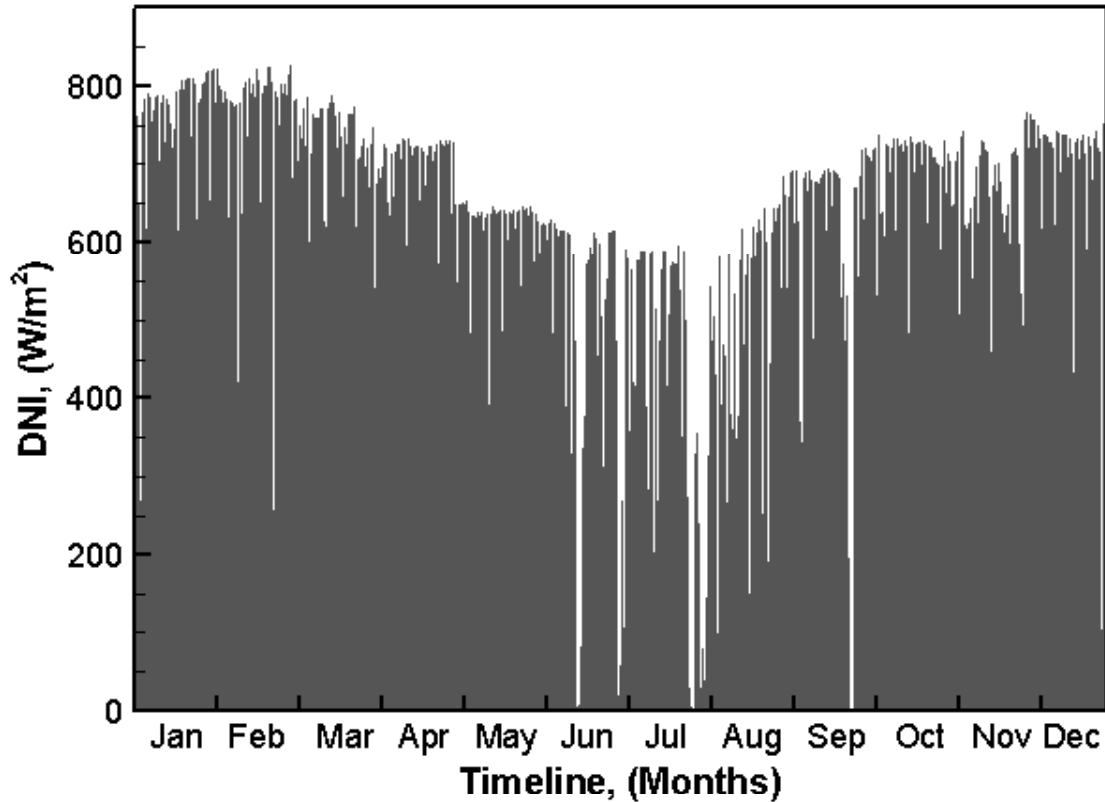


**Figure 4.5: Variation of DNI for all the months of a typical meteorological year.**

#### **4.5 Economic Parameters**

The capital cost of a 330 MWe supercritical coal-based power plant with a single unit is about 701 USD/kWe as per norms of CERC “order no: L-1/103/CERC/2012” (Jayaraman et al. 2012). The present study considers the same for economic analysis. The procedure implemented by Ramaswamy et al. (2012) is considered for calculating the capital costs of the integrated plant under study. The investment cost of SCHPP has two main components, i.e., DCC and ICC. The DCC includes costs of the power block, land, planning of the site, and solar field. While the ICC covers costs of “Engineering, Procurement & Construction”, “Project Management”, “Interest during Construction”, and Pre-operative expenses. The detailed procedure for evaluating DCC and ICC of integrated SCHPP is given in Table 4.3. The total capital cost for all studied options has been computed and presented in Table 4.4.

For evaluating the annualized cost of electricity ( $ACoE$ ) and the Levelized cost of electricity ( $LCoE$ ) generation, the procedure followed by Suresh et al. (2010) as described in Chapter-3 is adopted in this study. The discount rate is considered as 12%, and the power plant life is taken as 25 years. The plant capacity factor ( $PCF$ ) is taken as 0.85 and auxiliary power consumption ( $APC$ ) as 7.5%. The cost of fuel is considered as 36 USD/ton (Gupta and Srivastav 2010).

The cost of capital/unit ( $CC$ ), the capital recovery factor ( $CRF$ ), and the annualized capital cost ( $ACC$ ) per kW are computed using equations 3.31, 3.32, and 3.33, respectively, as mentioned in Chapter-3.

Net energy generated annually ( $P_{Net}$ ) and the fixed capital cost/unit ( $FCC$ ) are calculated using equations 3.34 and 3.35 of Chapter-3, respectively. In this study, the fixed operation & maintenance cost ( $FOM$ ) is considered as 2.5 % of the capital cost (Sathaye and Phadke 2006). The fixed O&M cost/unit, the cost of fuel/unit ( $C_F$ ), and the total variable cost/unit ( $C_V$ ) have been obtained using equations 3.36, 3.37, and 3.38, respectively. In the study, the variable O&M cost ( $C_{VOM}$ ) is considered as 0.0036 USD/kWh (Adibhatla and Kaushik 2017).

The effect of escalation in annual fuel and O&M cost using levelizing factor ( $LF$ ) is taken into account for calculating  $ACoE$ . The equations 3.39, 3.40, and 3.41, as described in Chapter-3, are used to determine the annualized cost of electricity generation ( $ACoE$ ), the equivalent discount rate with escalation ( $d_e$ ), and the levelizing factor ( $LF$ ), respectively. An escalation rate ( $e$ ) of 2% in variable cost and fuel/O&M-fixed is taken into account for economic investigation (Suresh et al. 2010). The Levelized fuel and O&M cost ( $C_L$ ), the Levelized Cost of electricity generation ( $LCoE$ ), and the simple payback period ( $SPP$ ) of the plant under study have been calculated using equations 3.42, 3.43, and 3.44, respectively.

**Table 4.3:**

**The methodology adopted for economic analysis of plant under study**

Item Description	Unit	Cost	Formula Used
<b>A. “Direct Capital Costs” (DCC)</b>			
<b>i. Solar</b>			
Land	USD/m <sup>2</sup>	2.44	$A_a \times LM_r \times \text{Land cost/unit area}$
Site Preparation	USD/m <sup>2</sup>	2.33	$A_a \times LM_r \times \text{Site preparation cost/unit area}$
<b>ii. Solar Field</b>			
Mirrors	USD/m <sup>2</sup>	51.79	$A_a \times \text{Mirror cost/unit area}$
Support Structure			$A_a \times \text{Cost of material \& fabrication per kg}$
Weight/aperture area	Kg/m <sup>2</sup>	19	$\times \text{support structure weight in kg per unit area}$
Fabrication	USD/kg	3.17	
Foundation	USD/m <sup>2</sup>	4.23	$A_a \times \text{Foundation cost/unit area}$
Absorber Tubes	USD/m	325	$\text{Total length of absorber tube}$ $\times \text{Cost/unit length}$
Swivel Joints	USD/unit	1479.67	$(A_a \times \text{Cost of swivel joint per unit})$ $/\text{mirror area per swivel joint}$
HTF	USD/litre	4.23	$\text{Cost of HTF per litre} \times \text{volume of HTF}$
HTF System	USD/m <sup>2</sup>	40.16	$\text{Cost of HTF sytem per unit area} \times A_a$
Hydraulic Drives & Electric Motors	USD/unit	2747.97	$\text{Cost/unit} \times \text{Total length of absorber tube/}$ $\text{Trough length for each drive unit}$
ECE System	USD/m <sup>2</sup>	21.14	$A_a \times \text{System cost/unit aperture area}$
<b>B. “Indirect Capital Costs” (ICC)</b>			
“Engineering, Procurement and Construction” (EPC) Cost		10% of DCC excluding land & site preparation cost	
“Project Management” (PM) Cost		5% of DCC excluding land & site preparation cost	
“Interest During Construction” (IDC)		$\text{DCC excluding land \& site preparation cost} \times$ $\text{debt (\%)} \times \text{debt cost} \times 0.5$	
Pre-Operative Expenses		$\text{DCC excluding land \& site preparation cost} \times$ $\text{debt (\%)} \times \text{debt cost} \times 0.01$	

\*Absorber tube length = [actual aperture area ( $A_a$ )/chord length]

\*Land to mirror area ratio ( $LM_r$ ) = 3.92

**Table 4.4:****Various costs related with economic analysis of plant under investigation**

Costs	Base Option	Replacement Scenarios		
		Option 1 (FWH #1)	Option 2 (FWH #2)	Option 3 (FWH #1+2)
<b>A. Direct Capital Cost (in Million USD)</b>				
<b>Power Block</b>	231.26	231.26	231.26	231.26
<b>Solar</b>				
Land	0	1.60	1.01	2.60
Site Preparation	0	1.52	0.96	2.49
Sub Total	0	3.12	1.97	5.09
<b>Solar Field</b>				
Mirrors	0	8.64	5.46	14.10
Support Structure	0	10.05	6.35	16.40
Foundation	0	0.71	0.45	1.15
Absorber Tubes	0	9.40	5.94	15.34
Swivel Joints	0	0.89	0.57	1.46
Hydraulic Drives & Electric Motors	0	0.53	0.33	0.86
ECE System	0	3.53	2.23	5.76
Sub Total	0	33.75	21.32	55.07
<b>Total Direct Capital Cost</b>	<b>231.26</b>	<b>268.13</b>	<b>254.55</b>	<b>291.42</b>
<b>B. Indirect Capital Cost (in Million USD)</b>				
EPC cost	23.13	26.50	25.26	28.63
PM cost	11.56	13.25	12.63	14.32
Interest during construction (IDC)	11.33	12.99	12.38	14.03
Pre-operative expenses	0.231	0.27	0.25	0.29
<b>Total Indirect Capital Cost</b>	<b>46.25</b>	<b>53.00</b>	<b>50.52</b>	<b>57.27</b>
<b>Total Capital Cost</b>	<b>277.51</b>	<b>321.13</b>	<b>305.07</b>	<b>348.68</b>

## 4.6 Results and Discussion

The main parameters of turbine bled steam and the reference plant's thermal performance parameters for different options considered in this study are given in Table 4.5. For the base case, the design energy efficiency of the 330 MWe CFPP is 34.17%. In power-boosting mode, the results presented in Table 4.5, Table 4.6, and Figure 4.6 showed that for Option-1 (Extraction steam to high-pressure FWH (*GJ1*) is replaced with solar energy), Option-2 (Extraction steam to high-pressure FWH (*GJ2*) is replaced with solar energy) and Option-3 (Extraction steam to both high-pressure FWHs (*GJ1* & *GJ2*) is replaced with solar energy) the improvement in energy efficiency over the base case is 7.14%, 3.86% and 11.32% respectively. And the improvement in exergy efficiency over the base case is 7.16%, 3.59%, and 11.34% for all three considered options, respectively. The improvement in energy and exergy efficiency for Option-2 is almost half of estimated for Option-1. This may be because, in Option-2, the steam saved (ton/h) and thus corresponding thermal energy saved is about 1.71 and 1.56 times less than Option-1, respectively. The biggest improvement in energy and exergy efficiency over the base case is obtained for Option-3 because, in this case, both high-pressure FWHs are replaced with solar energy, thus allowing more solar contribution.

In power boosting mode, the generator power output of the solar-coal hybrid power plant is increased from the generator's rated power output for all three options by 24/13/38 MW, respectively, and the solar collector area of about 16.69/10.54/27.23 ha is required for all three options considered in this study, respectively as presented in Table 4.7. The land requirement for the solar field is about three times the collector area (Pai 1991).

Figure 4.7 displays the variation of energy performance index (*EnPI*) and exergy performance index (*ExPI*) for all replacement options. From Figure 4.7, it can be clearly observed that the value of *ExPI* is greater than *EnPI* for all replacement options. Both *EnPI* and *ExPI* are maximum for Option-1, and it can also be seen that the highest *ExPI* is obtained



for Option-1. This distinctly indicates that the exergetic solar energy utilization for feedwater heating is higher than the energetic utilization of solar energy for feedwater heating. Therefore, it can be deduced that the utilization of solar energy for feedwater heating based on exergy is more efficient than that based on energy.

The percentage solar contribution and percentage power-boosting for all replacement options are shown in Figure 4.8. It can be seen from Figure 4.8 that the solar contribution for Option-3 is the highest (11.56%), followed by Option-1 (7.38%), and the solar contribution is the least for Option-2 (4.85%) because of obvious reason as stated above. The biggest improvement in power-boosting mode is witnessed for Option-3 (11.34%), followed by Option-1 (7.16%) and Option-2 (3.88%).

**Table 4.5:**

**Thermal performance parameters for various FWH replacement options**

Replacement Scenarios	Option 1 (FWH #1)	Option 2 (FWH #2)	Option 3 (FWH #1+2)	
			#1	#2
Steam saved (ton/h)	85.03	49.53	85.03	49.53
			134.56	
Steam Inlet Temperature (°C)	339.96	452.51	339.96	452.51
Steam Outlet Temperature (°C)	219.02	192.41	219.02	192.41
Steam Inlet Pressure (bar)	43.72	21.72	43.72	21.72
Thermal Energy Rate (kJ/h)	260132279	166524813	426657092	
Thermal Energy (MW)	72.26	46.26	118.52	
W <sub>Turbine</sub> (MW)	HP	89	89	
	IP	141	146	
	LP	129	138	
	Overall	359	373	
Cycle Efficiency, $\eta$ (%)	36.61	35.49	38.04	

**Table 4.6:****Energetic and Exergetic performance comparison of 330 MWe solar-coal hybrid power plant**

<b>Replacement Options</b>	<b>Power Boosting Mode</b>				
	<b>Gross power output (MWe)</b>	<b>Energy Efficiency (%)</b>	<b>Improvement over base case (%)</b>	<b>Exergy Efficiency (%)</b>	<b>Improvement over base case (%)</b>
Base Case	335	34.17	-	32.53	-
Option 1 (FWH #1)	359	36.61	7.14	34.86	7.16
Option 2 (FWH #2)	348	35.49	3.86	33.70	3.59
Option 3 (FWH #1+2)	373	38.04	11.32	36.22	11.34

**Table 4.7:****Performance indicators of the solar-coal hybrid power plant**

<b>Performance parameters</b>	<b>Replacement Scenarios</b>		
	<b>Option 1 (FWH #1)</b>	<b>Option 2 (FWH #2)</b>	<b>Option 3 (FWH #1+2)</b>
Net Heat Rate (kJ/kWh)	9832.36	10143.15	9463.31
Power Boosting (MW)	24	13	38
Solar Collector Area (m <sup>2</sup> )	166852.9	105409.2	272262.1
Solar Contribution (%)	7.38	4.85	11.56

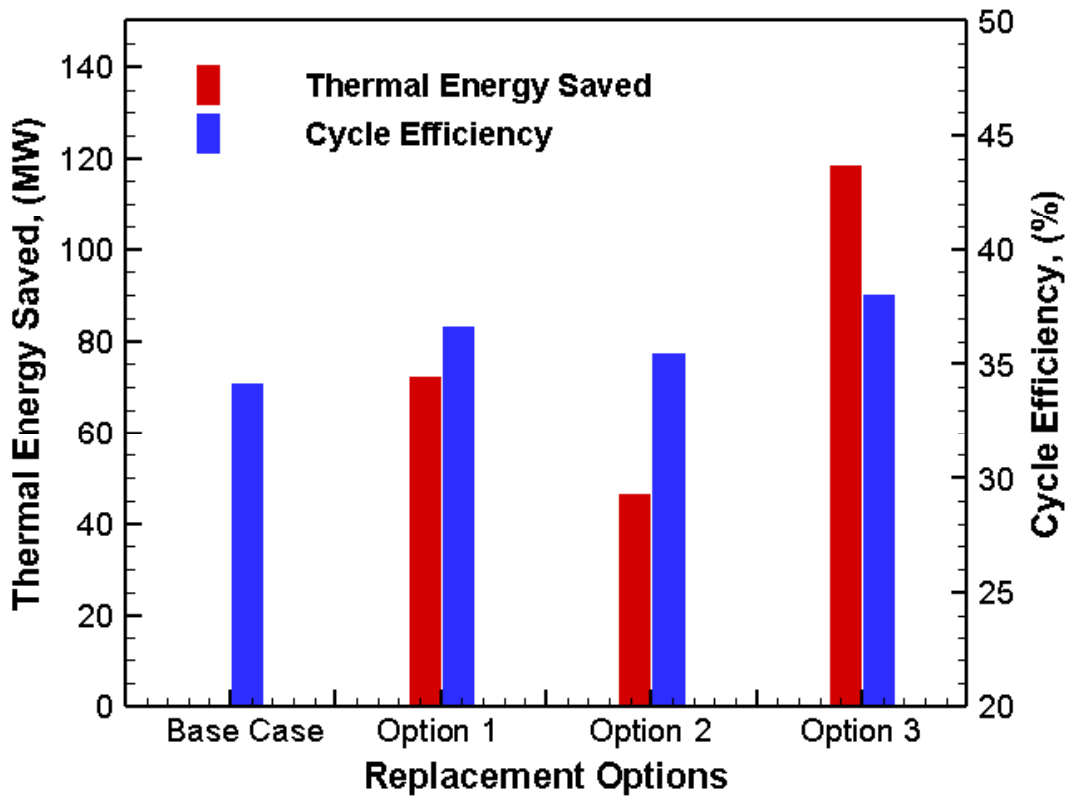


Figure 4.6: Thermal energy saved and cycle efficiency for different replacement options.

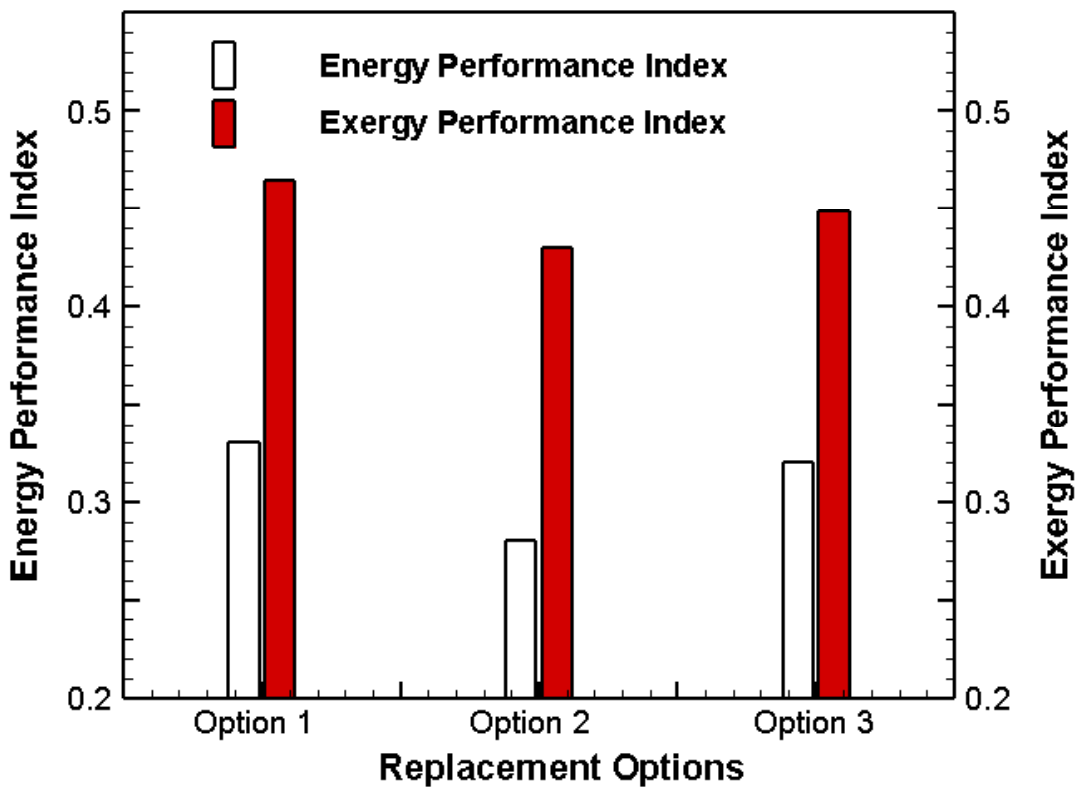


Figure 4.7: Energy performance and Exergy performance index for different scenarios.

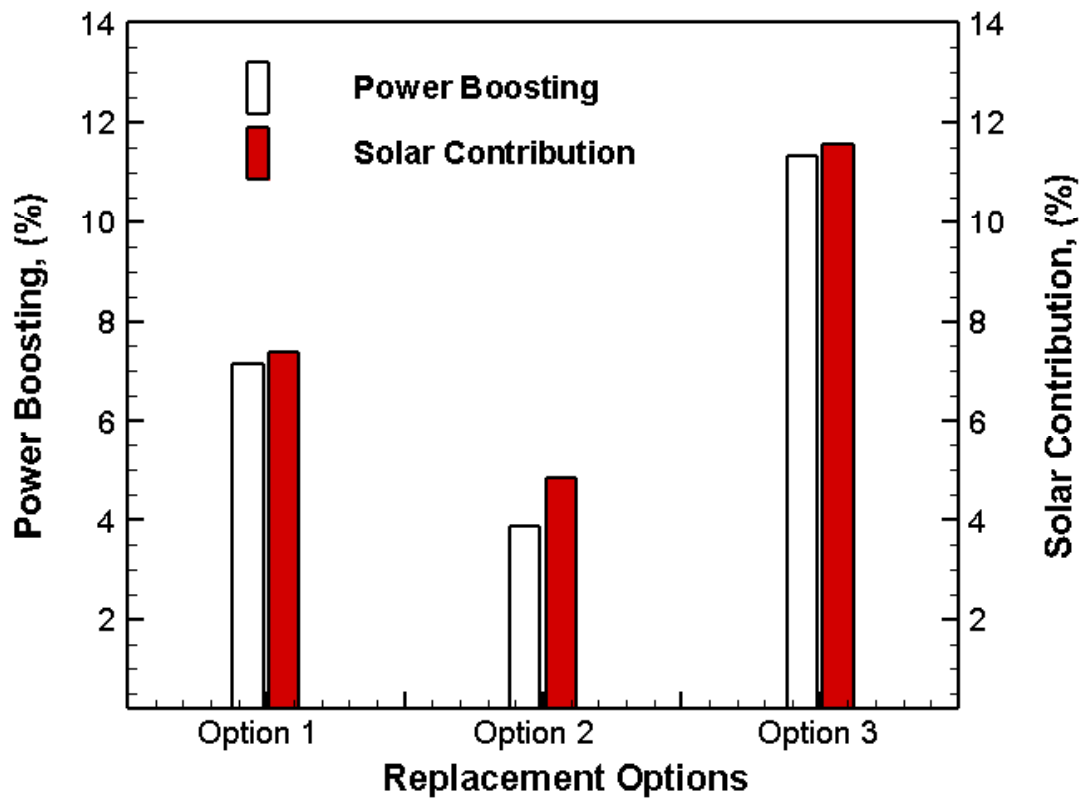


Figure 4.8: Power-boosting and solar contribution for different replacement options.

#### 4.6.1 Environmental analysis

The coal-based thermal power plants release various pollutants into the atmosphere and hence cause environmental degradation. Among these pollutants, CO<sub>2</sub> emissions are the major contributors to environmental pollution. Therefore, in the present investigation, solar energy is integrated under different scenarios into 330 MWe sub-critical coal-based TPP to reduce coal consumption and CO<sub>2</sub> emissions. In this study, the annual coal saving is calculated for all three options using thermodynamic energy analysis for solar-coal hybrid power plant (Fuel-saving approach). Corresponding to annual coal saving, the annual reduction in CO<sub>2</sub> emissions is evaluated using the methodology adopted by Sunil and Soni (Sunil and Soni 2019a, Sunil and Soni 2019b, Sunil and Soni 2020). The annual coal saving and annual reductions in CO<sub>2</sub> emissions for all three replacement options considered are shown in Figure

4.9. Option-1 results in annual coal saving and the corresponding reduction in CO<sub>2</sub> emissions of about 23856 tons and 47072 tons, respectively. For Option-2, the annual coal saving and the corresponding reduction in CO<sub>2</sub> emissions are 13584 tons and 26804 tons, respectively. In Option-3, the annual coal saving and the corresponding reduction in CO<sub>2</sub> emissions are 37104 tons and 73213 tons, respectively. This can be inferred from Figure 4.9 that the fuel-saving and reduction in CO<sub>2</sub> emissions are proportionate with the solar contribution for all three options discussed in this study.

#### **4.6.2 Economic analysis**

For economic analysis, the various economic parameters have been calculated using equations 3.31 to 3.44, as described in Chapter-3. The methodology is given in Table 4.3, and different costs associated with reference and hybrid plant given in Table 4.4 have been adopted for the economic investigation. The exhaustive economic analysis of the present study is given in Table 4.8. The results presented in Table 4.8 show that the increase in total capital costs (*TCC*) over the base case for Option-1 is 15.72%, for Option-2 is 9.93%, and for Option-3, it is 25.64%. The LCoE and SPP for all three replacement options are shown in Figure 4.10. Figure 4.10 shows that LCoE increases from the base case scenario to all three replacement options.

Similarly, the simple payback period also increases. The economic analysis results in Table 4.8 show that LCoE (USD/kWh) for the base Option and three replacement options are 0.0436/0.0452/0.0447/0.0463 and simple payback period (years) are 3.05/3.39/3.26/3.57, respectively. Considering the fuel cost as 36 USD/ton, the annual savings in the fuel cost are 0.86/0.49/1.33 million USD for Option-1, Option-2, and Option-3, respectively. The results of energetic, exergetic, environmental, and economic analysis discussed in the present

investigation are in agreement with the previous studies available in the literature (Suresh et al. 2010, Adibhatla and Kaushik 2017).

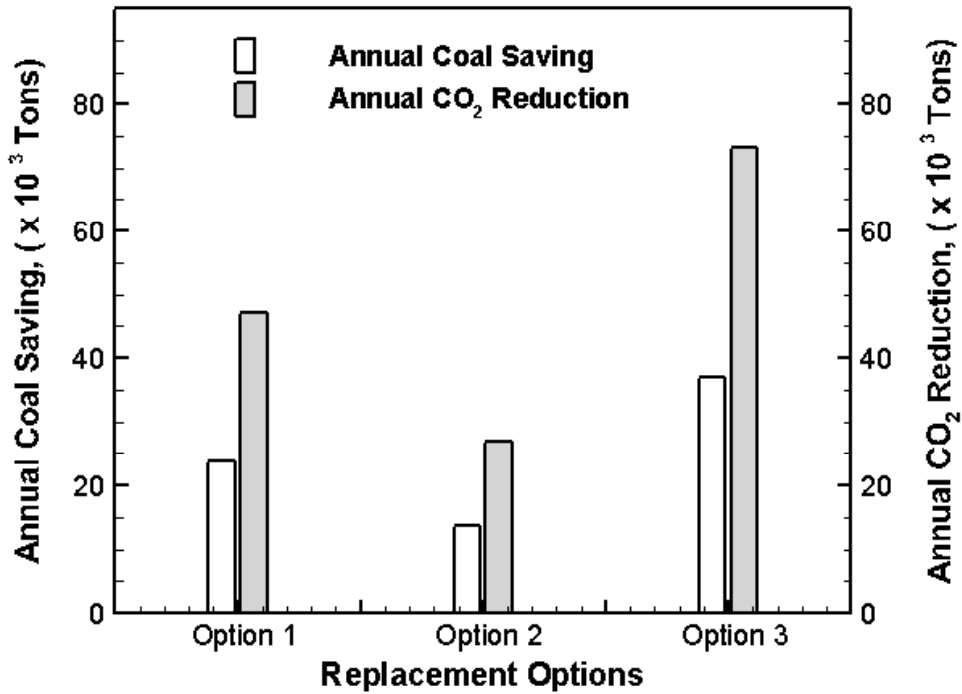


Figure 4.9: Annual coal saving and CO<sub>2</sub> reduction for various replacement options.

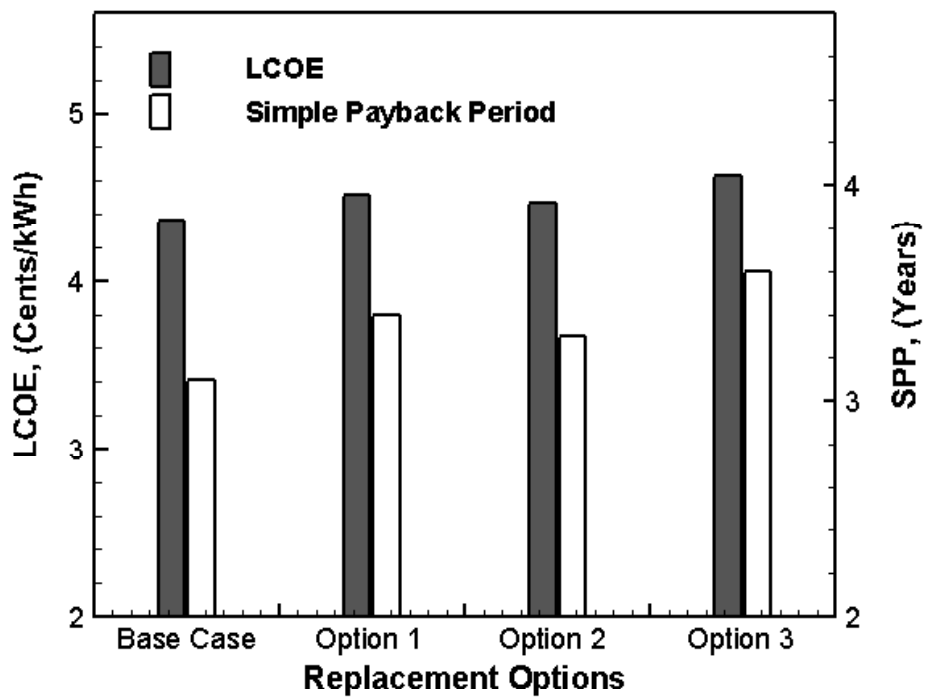


Figure 4.10: LCoE and SPP for different replacement options.

**Table 4.8:****Economic analysis of 330 MWe supercritical Solar-Coal hybrid power plant**

Item Description	Unit	Base Option	Replacement Scenarios		
			Option 1 (FWH #1)	Option 2 (FWH #2)	Option 3 (FWH #1+2)
Total Capital Cost	Million USD	277.51	321.13	305.07	348.68
Generator Power Output	MW	335	335	335	335
Capital Cost/Unit	USD/kWe	828.39	958.60	910.66	1040.84
Power Plant Life	Years	25	25	25	25
Discount Rate	Fraction	0.12	0.12	0.12	0.12
CRF	Fraction	0.13	0.13	0.13	0.13
ACC	USD/kW	105.62	122.22	116.11	132.71
Annually Net Energy Generated ( $P_{Net}$ )	kWh/kW	6887.55	6887.55	6887.55	6887.55
FCC/unit	USD/kWh	0.015	0.018	0.017	0.019
$C_{FOM}$ /unit	USD/kWh	0.0030	0.0035	0.0033	0.0038
GCV	kJ/kg	21767	21767	21767	21767
Net Unit Heat Rate ( $UHR_{Net}$ )	kJ/kWh	10536.76	9832.36	10143.15	9463.31
Fuel Cost ( $C_F$ )/unit	USD/kWh	0.0174	0.0162	0.0168	0.0156
$C_V$ /unit	USD/kWh	0.0210	0.0199	0.0204	0.0192
ACoE	USD/kWh	0.0394	0.0411	0.0405	0.0442
Escalation Rate (e)	Fraction	0.02	0.02	0.02	0.02
Equivalent Discount Rate with Escalation ( $d_e$ )	Fraction	0.098	0.098	0.098	0.098
LF	Fraction	1.17	1.17	1.17	1.17
Levelized Fuel and O&M Cost ( $C_L$ )	USD/kWh	0.0282	0.0274	0.0278	0.0270
LCoE	USD/kWh	0.0436	0.0452	0.0447	0.0463
SPP	Years	3.05	3.39	3.26	3.57

## 4.7 Summary

The 4-E analysis (energetic, exergetic, economical, and environmental) of a 330 MWe sub-critical coal-fired thermal power plant integrated with concentrated solar thermal energy is presented in this chapter. The integration of solar energy into the existing 330 MWe sub-critical coal-fired thermal power plant is done using three replacement options. The energetic analysis results show that the highest energy efficiency of 38.04% is attained for Option-3. Similarly, the results of exergetic analysis show that the highest exergy efficiency of 36.22% is attained for Option-3. The environmental analysis performed using the fuel-saving approach shows that the maximum reduction in coal consumption (37104 tons of coal) and CO<sub>2</sub> emissions (73213 tons of CO<sub>2</sub>) also corresponds to Option-3. This is because of the maximum solar contribution (11.56%) in Option-3.

Similarly, the annual saving in fuel cost (1.33 million USD) for Option-3 is the highest. In power boosting mode, the augmentation in generator power output is maximum for Option-3, followed by Option-1 and Option-2. The economic analysis results show that LCoE and simple payback period increase slightly with an increase in solar contribution. The simple payback periods for all replacement options are seemingly attractive. The investigation carried out in this chapter suggests that hybridization of coal-fired thermal power plants with solar thermal energy is a very lucrative alternative. Such hybridization will help mitigate climate change, environmental protection, and support developing countries in clean power generation and achieve sustainable development goals.